03.1

Correlation between the abnormal enhancement of the separated flow and extraordinary pressure drops in the groove on the plate when the angle of inclination changes from 0 to 90°

© S.A. Isaev[1,2], S.V. Guvernyuk[3], D.V. Nikushchenko[1], A.G. Sudakov[2], A.A. Sinyavin[3], E.B. Dubko[2]

[1] State Marine Technical University, St. Petersburg, Russia
[2] St. Petersburg State University of Civil Aviation, St. Petersburg, Russia
[3] Institute of Mechanics of Lomonosov Moscow State University, Moscow, Russia
E-mail: isaev3612@yandex.ru

Received March 17, 2023
Revised May 10, 2023
Accepted June 5, 2023

A numerical and physical study of the air turbulent flow around a plate (with a long inclined groove of a moderate depth which has hemispherical ends) has been performed at the Reynolds number of $6.7 \cdot 10^4$ which is determined by the width of the groove. The groove inclination angle with respect to the oncoming flow varies from 0 to 90°. The stationary near-wall flow of incompressible viscous medium was simulated by solving the Reynolds-averaged Navier–Stokes equations closed using the shear stress transport model. The static pressure distributions in single grooves were measured in a wind tunnel at the Institute of Mechanics of Moscow State University. There was determined a groove inclination angle at which the abnormal enhancement of the separated flow is observed. The resulting extraordinary pressure drops in the grooves were in a good agreement with ultrahigh absolute values of negative relative friction. Velocities of the return and secondary swirl flows turned out to be comparable with the oncoming flow velocity.

Keywords: separated flow, inclined grooves, plate, abnormal enhancement, numerical simulation, wind tunnel experiment.

DOI: 10.61011/TPL.2023.08.56684.19560

The phenomenon of abnormal enhancement of the separated turbulent flow and heat transfer in moderate-depth grooves inclined at the angle of 45° was recently discovered by numerical simulation methods; it was presented for the first time in [1] for the case of one-row sparse packages of grooves in the stabilized hydrodynamic section of a narrow channel. Maximum absolute values of negative friction and heat flux in the middle longitudinal section at the groove bottom in the return flow region is manyfold (up to 4–6 times) higher than respective characteristics at the plane-parallel channel wall. Maximal values of the return-flow velocity Cartesian components are close to the mass-average flow velocity in the channel, while those of the secondary (swirl) flow in the groove exceed this mass-average flow velocity by 1.23 times. At the same time, the relative (to that of the plane-parallel channel) heat removal from the groove-containing area exceeds relative hydraulic losses (1.7 against 1.45). In [2] there was numerically shown that abnormal enhancement of the separated and swirl flows in the groove radically depends on the sparse-package groove inclination angle at the narrow channel wall in the stabilized hydraulic section. In the angle variation range of 40 to 60°, a three– or four-fold decrease in the relative negative friction is observed. Review [3] pays especial attention on identifying the mechanism of the separated flow and heat transfer abnormal enhancement in the inlet parts of single and one-row inclined grooves. That mechanism is associated with arising of extraordinary pressure drops between the zones of stagnation on the groove windward side and areas of negative pressure in the core of self-organized tornado-like vortices. These pressure drops cause ultrahigh velocities of return, secondary, upward and downward flows, as well as a manyfold (from 1.5–2 to 5–7) increase in relative friction and heat fluxes at the groove bottom as compared to those during flowing around the plane wall. Experimental investigation of single and packaged grooves are reported in [4–6]. The numerically revealed phenomena were confirmed by using facilities of the MSU Institute of Mechanics and Kazan Research Center of RAS where static pressure drops in single grooves on the plate were measured by varying the inclination angle from 0 to 90° at high Reynolds numbers; in addition, velocity fields of the laminar and turbulent air flows in narrow channels with two-row inclined grooves were measured [4]. This paper is focused on establishing an interrelation between abnormal enhancement of the separated flow in moderate-depth single grooves on the plate and extraordinary static pressure drops in the inclination angle θ measurement range of 0 to 90°.

The near-wall turbulent low-velocity air flow around the plane plate with an inclined groove located on it

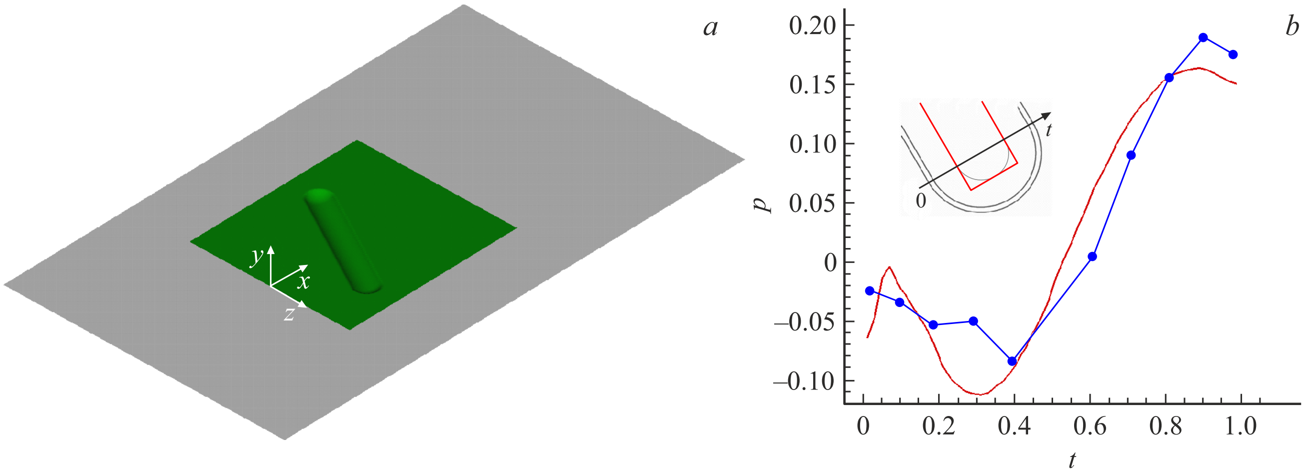

Figure 1. Schematic view of a groove on the plate in the case of inclination angle of 60° (a), and comparison of calculations and experimental results in the case of $\theta = 40°$ (b).

(Fig. 1, a) will be calculated based on the Reynolds-averaged Navier–Stokes equations (RANS) closed using the Menterś Shear Stress Transport model (MSST) [7]. The set of initial stationary equations in the linearized form will be solved using multiblock computing techniques and partially intersecting different-scale structured grids [1–4]. Algebraic equations will be solved by the preconditioned BiCGSTAB method [8] using the algebraic multigrid accelerator from the Demidov library (AMGCL) [9] for correcting the pressure and ILU0 for other variables. The Reynolds number will be determined based on characteristic uniform flow velocities U and groove width D: $\mathrm{Re} = UD/\nu = 6.7 \cdot 10^4$, where ν is the air kinematic viscosity.

The streamlined plate with a groove is a rectangular segment of a plane wall 22 long and 12.3 wide. The center of a groove 6 in length and 0.25 in depth is located at the distance of 9.5 from the inlet cross-section where the uniform flow gets formed and transforms near the wall into a developing boundary layer with the preset thickness of 0.17. The computational domain will be arranged on the rectangular segment of the plate and have the vertical size of 7.3. The rounding radius of the groove edge is assumed to be 0.02. The Cartesian frame of reference x, y, z will be placed in the beginning of the groove-containing segment (see Fig. 1, a). U, V, W are the Cartesian velocity components. Distributions of relative friction f/f_{pl} (where f_{pl} is defined at the plane wall) and static pressure p normalized to the double velocity head will be considered in the frame of reference s, y, t related to the inclined groove. Profiles of the velocity longitudinal component in the fixed frame of reference $Q = U\cos\theta + W\sin\theta$ will be calculated in the middle of the characteristic cross-section at the place where the groove spherical segment and cylindrical trench join each other.

The multiblock grid consisting of four fragmentary grids contains about 5.85 mln cells. Boundary conditions for calculations are imposed in the same way as in [1–4]. On the lateral and top boundaries of the computational domain slip conditions are specified; soft boundary conditions are set at the outlet boundary, no-slip conditions are set at the wall. The uniform flow turbulence intensity at the inlet boundary is chosen equal to 0.5% as in the experiment [4]; the turbulence scale is taken equal to characteristic size D.

Fig. 1, b illustrates the comparison of distributions of measured static pressure p normalized to the double velocity head with numerical predictions obtained in the framework of the MSST-based RANS approach in the characteristic cross-section of the groove inclined at angle $\theta = 40°$. Quite satisfactory agreement between the data confirms the acceptability of the developed calculation concept. Note also the existence of extraordinary static pressure differences between the peak pressure on the windward side and minimum negative pressure at the groove bottom in the region of development of the swirl tornado-like flow.

The effect of the groove inclination angle on enhancement of transport processes inside the groove is illustrated in Fig. 2. There is considered the evolution (with varying θ from 0 to 90° with the step of 10°) of distributions of relative friction $f/f_{pl}(s)$ in the longitudinal middle section and profiles of static pressure $p(t)$ in the characteristic transverse section. The range of inclination angle θ, where a significant (by 1.5–2 times) decrease in minimal f/f_{pl} is observed, equals 40 to 70° (Fig. 2, a). When θ varies from 0 to 30°, the unseparated flow-through flow in the moderate-depth long groove transforms into a swirl flow. When $\theta = 30°$, $(f/f_{pl})_{\min} = -1.15$ which is almost twice lower than at $\theta = 0°$. Further increase in θ is characterized by conversion of the bell-shaped $f/f_{pl}(s)$ distribution to the distribution with two monotonically decreasing bulges; as θ increases, the second bulge shifts towards the groove inlet. The $(f/f_{pl})_{\min}$ value gets reached at $\theta = 50°$ and appears to be close to -2. Above 70°, the return flow intensity in the separation zone decreases, though $(f/f_{pl})_{\min}$ remains significantly high and close to -1 at $\theta = 90°$.

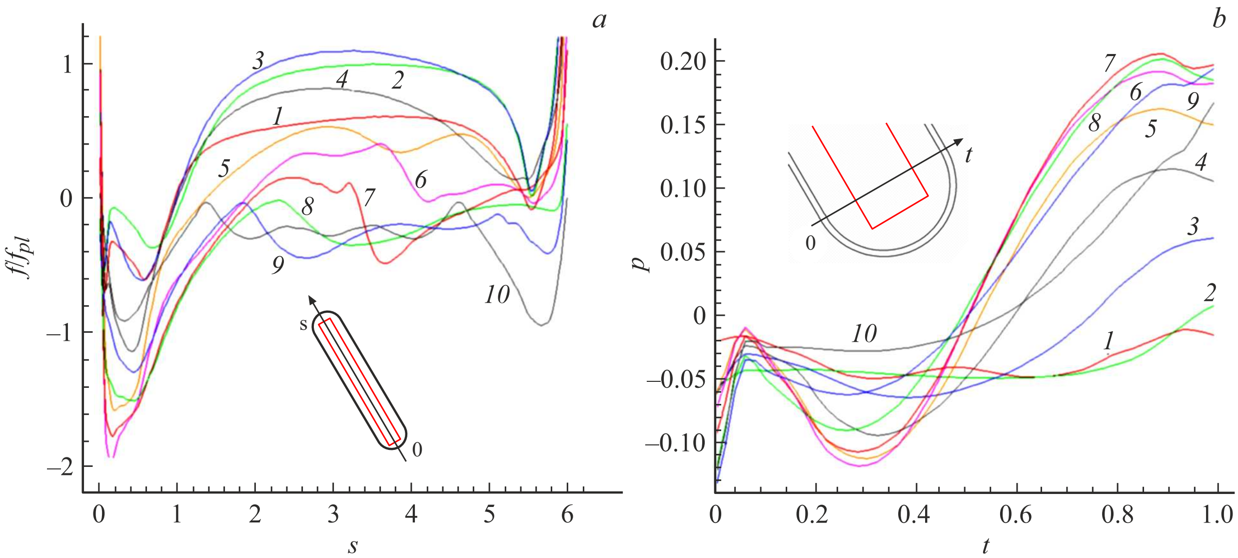

Figure 2. The effect of inclination angle θ on the distributions of relative friction $f/f_{pl}(s)$ in the groove longitudinal section (*a*) and static pressure $p(t)$ in the cross-section of transition from the inlet spherical segment to the cylindrical trench (*b*). $\theta = 0$ (*1*), 10 (*2*), 20 (*3*), 30 (*4*), 40 (*5*), 50 (*6*), 60 (*7*), 70 (*8*), 80 (*9*) and 90° (*10*).

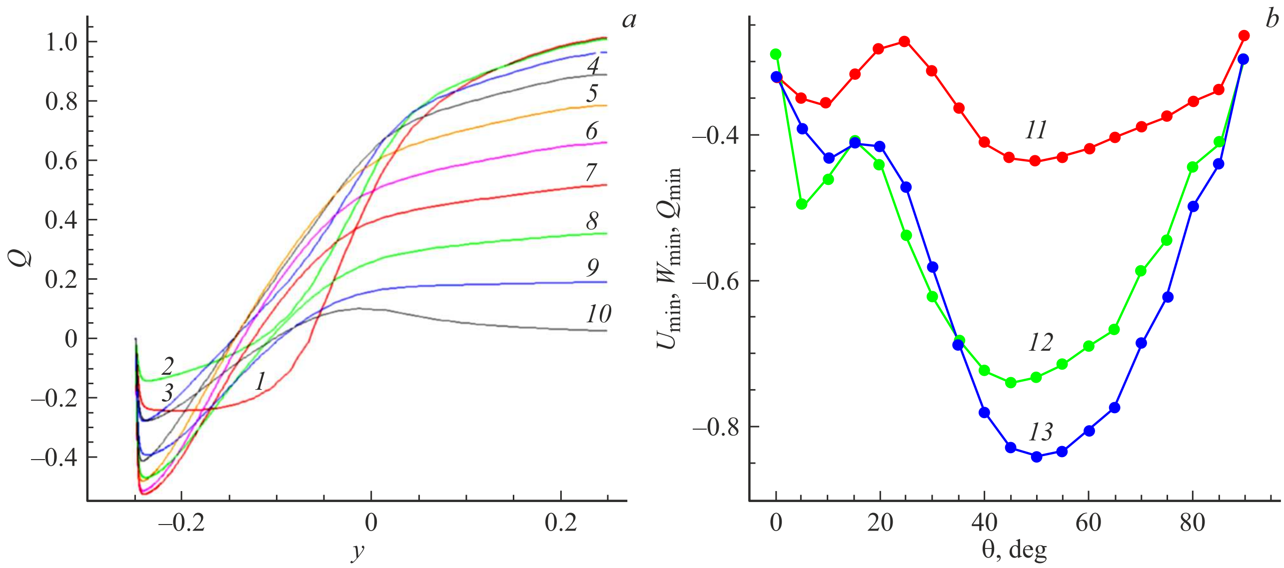

Figure 3. *a* — the effect of inclination angle θ on the evolution of velocity component profiles along s in the fixed frame of reference: $\theta = 0$ (*1*), 10 (*2*), 20 (*3*), 30 (*4*), 40 (*5*), 50 (*6*), 60 (*7*), 70 (*8*), 80 (*9*) and 90° (*10*). *b* — the effect of inclination angle θ on extremal characteristics $U_{\min}$ (*11*), $W_{\min}$ (*12*) and $Q_{\min}$ (*13*).

Changes in the profiles of static pressure in the characteristic transverse section of the groove inlet part (see Fig. 2, *b*) with varying the inclination angle from 0 to 90° make evident the interrelation between the pressure drop and structure rearrangement of the vortex flow in a single groove on the plate. The pressure drops across the groove are insignificant at low θ, though at 10° there arises a pressure peak at the windward edge, which reaches 0.15−0.2 with further increase in θ to above 40°. When θ changes from 20 to 30°, a zone of negative pressure (of about −0.09) emerges in the downwind part. When θ exceeds 40°, dimensions of that zone remain almost the same, and $p_{\min}$ reaches −0.12 at $\theta = 50°$. The maximum pressure drop between the stagnation zone at the groove windward side and low-pressure zone in the downwind groove part appears to be about 0.33 in case of abnormal enhancement of the separated flow.

The groove turning from the flow-wise direction to that transverse to the external flow radically changes the vertical structure and intensity of the flow in the groove inlet part (Fig. 3). A sharp change is observed in the separated flow profiles $Q(y)$ presented in Fig. 3, *a* in the range of 0 to 20°; therewith, the zero-velocity point approaches the groove bottom. This transformation of the velocity profile is associated with self-organization of the tornado-like vortex structure, which results in development of the swirl flow and formation in the groove of the near-bottom return flow that gets enhanced with increasing θ. $Q_{\min}$ reaches a value of about -0.5 at $\theta = 50-60°$.

Numerical forecasts for $U_{\min}$ and $W_{\min}$ enabled estimating extremal values of the return flow as $Q_{\min} = U_{\min}\cos\theta + W_{\min}\sin\theta$ (Fig. 3, b). The maximum absolute velocity appears to be close to the characteristic velocity of the external flow. In the θ range of 35 to 70°, $Q_{\min}$ appears to be lower than -0.7.

Thus, the numerically and experimentally established extraordinary static pressure drops in a single inclined groove on the plate, which take place during a turbulent airflow around the plate, are associated with ultrahigh absolute values (of about $1.5-2$) of relative friction in the middle section at the groove bottom at inclination angles of 35 to 70°. Extremal values of velocities of the return and secondary swirl flows in the groove proved to be comparable with the oncoming flow velocity.

Financial support

The study was supported by the Russian Science Foundation (project 22-19-00056).

Conflict of interests

The authors declare that they have no conflict of interests.

References

[1] S. Isaev, M. Gritckevich, A. Leontiev, I. Popov, Acta Astronaut., **163**, 202 (2019). DOI: 10.1016/j.actaastro.2019.01.033
[2] S.A. Isaev, A.B. Mazo, D.V. Nikushchenko, I.A. Popov, A.G. Sudakov, Tech. Phys. Lett., **46** (11), 1064 (2020). DOI: 10.1134/S1063785020110073.
[3] S.A. Isaev, Fluid Dyn., **57** (5), 558 (2022). DOI: 10.1134/S0015462822050081.
[4] S.A. Isaev, A.I. Leontiev, E.E. Son, S.V. Guvernyuk, M.A. Zubin, N.I. Mikheev, I.A. Popov, D.V. Nikuschenko, A.G. Sudakov, J. Phys.: Conf. Ser., **2088**, 012018 (2021). DOI: 10.1088/1742-6596/2088/1/012018
[5] M.A. Zubin, A.F. Zubkov, Fluid Dyn., **57** (1), 77 (2022). DOI: 10.1134/S0015462822010128.
[6] V.I. Terekhov, V.V. Terekhov, I.A. Chokhar, N. Yan Lun, Teplofizika i aeromekhanika, **29** (6), 935 (2022). (In Russian)
[7] F.R. Menter, in *23rd Fluid Dynamics, Plasmadynamics, and Lasers Conf.* (Orlando, USA, 1993), paper AIAA-93-2906. DOI: 10.2514/6.1993-2906
[8] Y. Saad, *Iterative methods for sparse linear systems*, 2nd ed. (Society for Industrial and Applied Mathematics, Philadelphia, 2003).
[9] D. Demidov, *AMGCL*: C++ *library for solving large sparse linear systems with algebraic multigrid method* [Electronic source]. URL: http://amgcl.readthedocs.org/

Translated by Solonitsyna Anna